Usage of the Internet Resources for Research of the Ionosphere and the Determination of Radio Wave Propagation Conditions

Olga Maltseva

Institute of Physics Southern Federal University, Stachki, 194, Rostov-on-Don, Russia
mal@ip.rsu.ru

Abstract: In the field of ionospheric research is impossible to obtain the new results, new knowledge without use of Internet resources. The paper provides examples of the use of these resources on the basis of generalization and complement to reports made on the three previous ICTRS conferences. Results are presented in four areas of possible data: (1) vertical sounding, (2) total electron content TEC, measured by high orbit navigation satellites, (3) plasma frequencies measured by low orbit satellites, (4) empirical models of the ionosphere. The main achievement in the first direction is the creation of GAMBIT, designed to provide global maps of ionospheric parameters foF2 and hmF2 with delay of 15 minutes in relation to real time. The estimation of conformity of the IRI model to experimental data of foF2 for high-latitude station of southern hemisphere is made. Within the second direction the effectiveness coefficient of use of the observational median of the equivalent slab thickness in comparison with thickness of the IRI model is introduced. It is shown that this coefficient almost always exceeds 1, reaching values 1.5-2 globally. Behavior features of deviations of calculated foF2 from observational values during the strongest geomagnetic disturbances of April 2014 and March 2015 are given. In the framework of the third direction validation of a plasmaspheric part of a N(h)-profile according to satellite IMAGE data is performed. It was concluded that to disambiguate N(h)-profiles it is necessary to improve both values of TEC, and the shape of the topside part because the plasmaspheric part is close to existing model RPI. Within the fourth direction the statistics of comparisons of various models was increased including high-latitude region of the southern hemisphere.

1 INTRODUCTION

Internet affects the lives of every person, providing huge opportunities in the information sphere. This paper describes the opportunities associated with databases for ionospheric research. To solve many scientific and technological problems need to know the conditions in the ionosphere, within which there are the satellites that provide us, in turn, information about the state of the ionosphere. This article points out the most important databases and displays the results of their use. Possibilities of use of Internet data are illustrated with examples: (1) vertical sounding (VS), (2) global maps of the total electron content of the ionosphere TEC, (3) data satellites CHAMP and DMSP, and (4) the International Reference Ionosphere model IRI. Each of these areas corresponds to a separate section (2-5).

2 INTERNET POSSIBILITIES OF USAGE OF THE VERTICAL SOUNDING DATA

In the 20th century, the key parameter of the ionosphere was the peak concentration NmF2 (or critical frequency foF2), measured by special receiver-transmitters - ionosondes. By the end of the 20th century, digisondes, being ionosondes with automatic processing of samples, have been appeared when the need of the ionospheric data in real time and on a global scale has required to automate this process. A lot of programs have been created. System ARTIST for which now already the fifth version (Reinisch et al., 2009) was developed is most widely used. However, as shown by means of special expert program QualScan estimating quality of ionograms, usually 1/3 of digitized ionograms can be rejected (McNamara, 2006). The most promising is a new principle, which underlies dynasonde

(Zabotin et al., 2005) and provides the most accurate determination of the parameters of the ionosphere. The evaluation of improvements of ionospheric parameters determination by dynasonde in comparison with digisonde (ionosonde) was held in the paper (Maltseva et al., 2007). The most important are results for foF2 and hmF2. Figure 1 from this paper is an example of difference between automatic methods of determination of daily dependence of frequency foF2 by various methods of sounding: digisonde (method POLAN (P)) and dynasonde (method NeXtYZ (N) (Zabotin et al., 2005)) in comparison with the IRI model.
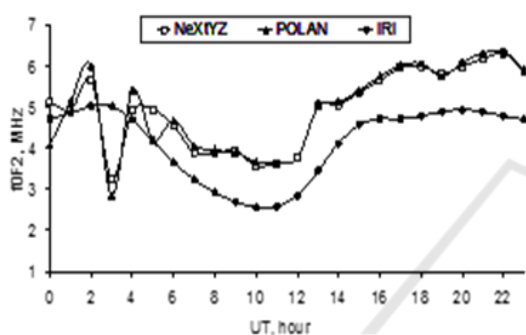
Figure 1: An example of differences between methods of foF2 determination: digisonde (method POLAN (P)) and dynasonde (method NeXtYZ (N)).

Table 1 shows the quantitative evaluation of absolute differences between critical frequencies obtained by these methods and the values of the IRI model. Results are shown for stations having dynasonde and for those days which had simultaneous measurements. The first column contains name of stations. The second column shows the month. The third column points out number of day when there were measurements. P-IRI column shows the difference between the method POLAN and the IRI model, N-IRI shows the difference between the method NeXtYZ and the IRI model, N-P column shows the difference between the methods NeXtYZ and POLAN. Values of P-IRI and N-IRI are an estimate of improving the determination of foF2 using experimental data. Values N-P are an estimate of improving the determination of foF2 by method NeXtYZ (dynasonde) compared with method POLAN (digisonde). If you take the average value of foF2 approximately 5 MHz, the improvement is 11-14%.

Table 1: Improvement of foF2 determination by new dynasonde.

station	month	Number of days	$|\Delta foF2|$, MHz		
			P-IRI	N-IRI	N-P
Lycksele	July	16	0.64	0.62	0.16
Tromso	July	16	0.57	0.59	0.19
BearLake	July	5	0.74	0.72	0.18
Tromso	Nove	3	0.6	0.6	0.10
Lycksele	April	5	0.83	0.76	0.14
Tromso	April	6	0.69	0.66	0.17

Figure 2 shows the difference between automatic methods of determining the values of hmF2, calculated by different methods of sounding: digisonde (method POLAN (P)) and dynasonde (method NeXtYZ (N)). Also values of hmF2 for the IRI model are given.
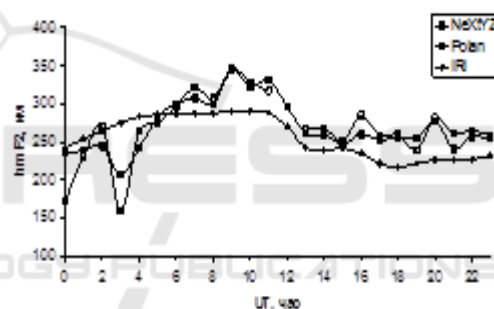
Figure 2: An example of differences between values of hmF2 obtained by various methods of sounding: digisonde (method POLAN (P)) and dynasonde (method NeXtYZ (N)).

Table 2 shows the quantitative evaluation of these differences (Maltseva et al., 2007). P-IRI column shows the difference between the method POLAN and the IRI model, N-IRI shows the difference between the method NeXtYZ and the IRI model, N-P column shows the difference between the methods NeXtYZ and POLAN.

As well as in a case with parameter foF2, values P-IRI and N-IRI characterize improvement in adapting the model to the experimental values of hmF2. N-P values have improved the definition of the maximum height by the new method. These values are significantly higher than the accuracy of measurement. Using as the mean value of hmF2 250 km we obtain approximately 15% improvement.

Table 2: Improvement of hmF2 determination by new dynasonde.

station	month	Number of days	$|\Delta hmF2|$, км		
			P-IRI	N-IRI	N-P
Lycksele	July	16	40.6	38.5	34.3
Tromso	July	16	48.5	44.7	29.2
Bea Lake	July	5	47.8	53.2	25.2
Lake	Novem	3	49.2	40.5	33.7
Tromso	April	5	20.3	20.5	24.5
Lycksele	April	6	29.5	19.2	29.7

Unfortunately, the stations equipped by dynasonde are not a lot. Data of other stations are collected in the form of multiple databases (GIRO, SPIDR, DIAS et al.) which are freely available, include data from several cycles of solar activity, and are permanently being updated and modified. A large contribution to this update provide reports from conference (URSI, 2015), in particular, the system GIRO was modified in GAMBIT (https://git.giro.uml.edu), which represents the global maps of foF2 and hmF2 delayed at least 15 minutes, compared with real time. The European System of DIAS was supplemented with the data of such stations as Moscow and Tromso.

3 INTERNET POSSIBILITIES OF USAGE OF THE TOTAL ELECTRON CONTENT OF THE IONOSPHERE

Despite the fact that, apparently, the method of the VS can be considered the best method for measuring the ionospheric parameters, its main deficiencies are rare network and quite often data gaps on some stations. In the 21st century, with the development of network of navigation satellites has been a shift to the identification of the total electron content (TEC) of the ionosphere as the main parameter, and even proposed to replace the parameter NmF2. The advantages of this option is its continuous monitoring, the availability of online databases of global maps for a period longer than the cycle of solar activity, information about the N(h)-profile. In (Maltseva et al., 2012; 2013; Maltseva, 2014) the TEC parameter was used to determine foF2 with experimental median of ionospheric equivalent slab thickness τ(med). Much more conformity of the

calculated values of foF2 with measurements in comparison with conventionally used value τ(IRI) (McNamara, 1985; Houminer, Soicher, 1996; Gulyaeva, 2011) was obtained. The improvement is achieved by taking into account a big difference between what was (τ(IRI) = TEC(IRI)/NmF2(IRI), NmF2(calc) = TEC(obs)/τ(IRI)), and what became (τ(med) = med(TEC(obs)/NmF2(obs)), NmF2(calc) = TEC(obs)/τ(med)). Illustration of this difference for the reference station Juliusruh is shown in Fig. 3. In this paper we introduce the efficiency factor Keff of using τ(med) compared with τ(IRI), and give the results of its determination for the individual stations in the various regions of the world and globally. Keff factor is defined as the quotient of the absolute deviations $|\Delta foF2|$ of calculated foF2 from the experimental values using these two parameters τ(IRI) and τ(med). Fig. 4 shows the coefficients for the 6 stations: the European mid latitude Juliusruh station, the American mid latitude Goosebay station, the American high-latitude station Thule in the northern hemisphere, the equatorial Ascension Island station, the low-latitude and high-latitude Grahamstown and Mawson stations of the Southern hemisphere. For comparison, the value of K=1 is displayed. Integrated characteristics are given in Table 3.
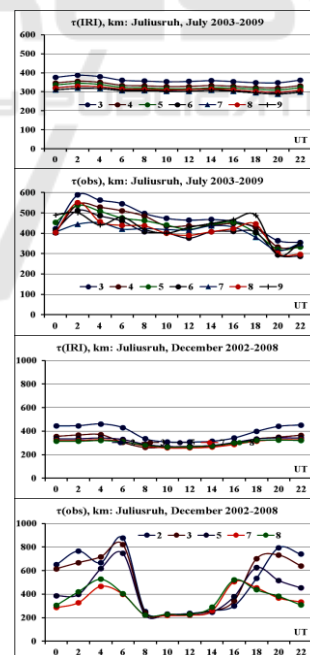
Figure 3: Differences between used values τ(IRI) and τ(med) on an example of the long-year data for July and December and the Juliusruh station.
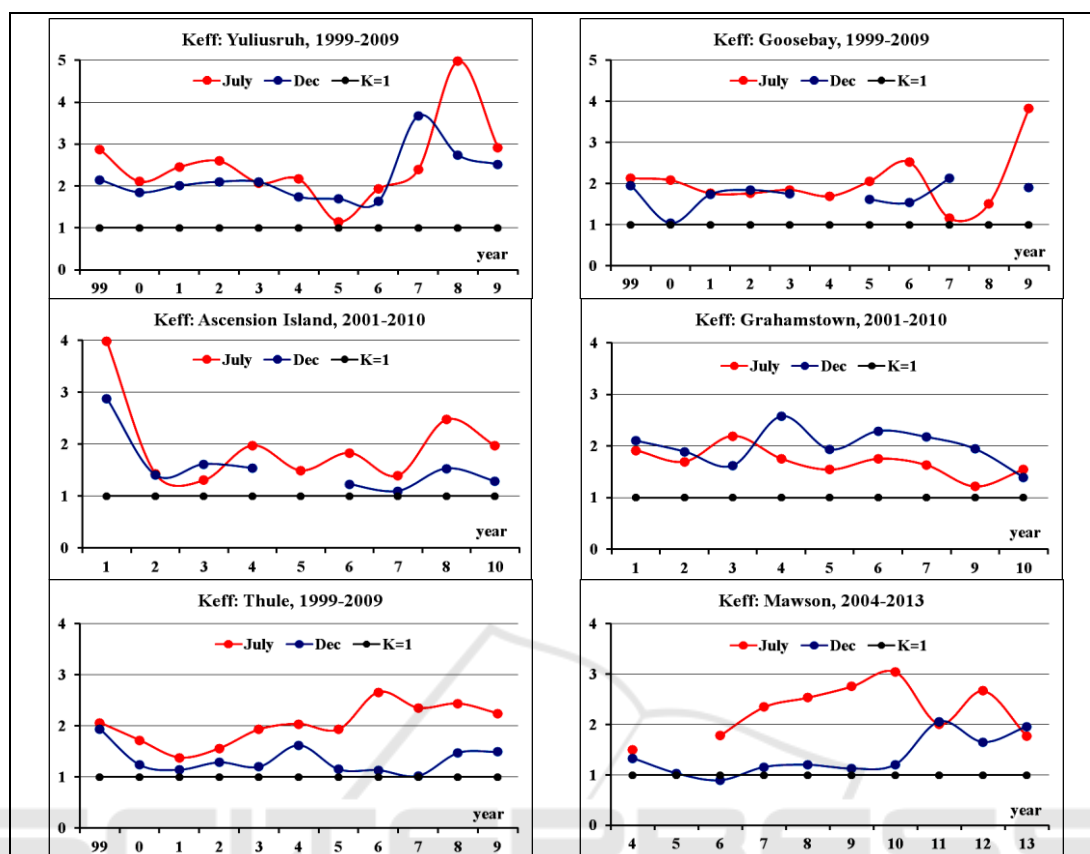
Figure 4: Coefficients Keff in various regions of the globe.

Table 3: Conformity averaging for all years between the calculated and observed values of foF2: coefficients Keff and the relative deviations σ (foF2), %

	σ(foF2), %							
	July				**December**			
station	Keff	med	ins	τ	Keff	med	ins	τ
Juliusruh	2.52	9.82	15.03	6.91	2.20	13.30	17.68	8.45
Goosebay	2.03	9.41	15.46	9.36	1.72	13.54	17.61	11.36
Thule	2.03	11.46	15.43	8.46	1.34	10.41	18.21	13.91
Grahams	1.70	9.53	15.84	10.09	1.99	12.44	17.26	9.40
Ascension	1.98	23.40	27.21	14.89	1.57	13.04	17.52	12.45
Mawson	2.26	44.26	48.83	25.7	1.36	15.28	24.82	20.75

It can be seen that the efficiency factor is close to 2 for July, i.e. results are in 2 times better, and near 1.5 for December. The same can be said about the relative deviation σ(foF2),%. With the exception of the Antarctic station Mawson deviations for τ(med) lie within 10%. Keff has been calculated globally for months with disturbances. Figure 5 shows the average monthly variations depending on the latitude for τ(IRI) (green triangles). For τ(med) red dots show results for the global map JPL. Figure 5 also includes the efficiency factors. Blue circles in all Figures show results of comparison of model IRI values with experimental medians for an illustration of accuracy of the model in relation to measurement.
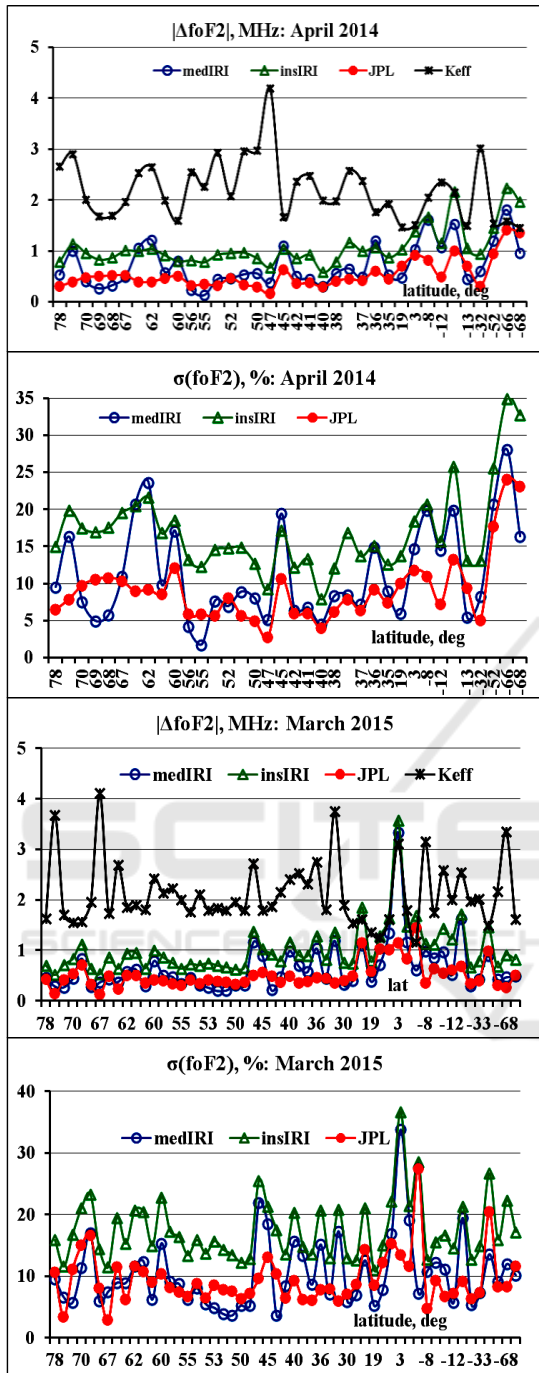
Figure 5: Behavior of Keff on a global scale.

Keff is close to 2 around the globe, and σ is less than 10% with the exception of the stations of the Southern hemisphere. This indicates that the simulation situation for the southern hemisphere has problems. For these months, the details of the comparison of deviations have been identified in

disturbed periods. Fig. 6 shows the Dst-index for these months (http://wdc.kugi.kyoto-u.ac.jp/dstdir/).
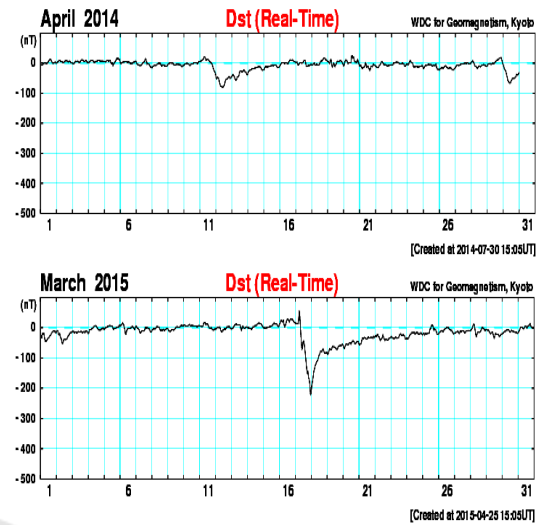
Figure 6: Behavior of Dst-indexes in months with disturbances

The behavior of Dst-index specifies which days had the greatest disturbances. In April 2014 this day is 12. In March 2015 these are 17-19 because disturbance was stronger. Fig. 7 presents the global results for specific days. In both cases values are also given for the quiet days preceding the disturbances. Two top figures show the results for τ(IRI), the lower - for τ(med), and these charts include in addition the values for τ(IRI), averaged over the 5 days considered.

We see that deviations for τ(IRI) are maximum in disturbed days. In the southern hemisphere still get big deviations also for τ (med). To conclude this Section it is necessary to say a few words about the alternatives. In recent years, assimilation techniques become widespread (e.g. Khattatov et al., 2005; Fuller-Rowell et al., 2006), in which N(h) -profile of the ionosphere is fitted by the very powerful methods so that it satisfies the measured TEC(obs), but emphasis on the determination of foF2 was not done. And when compared with measurements by ionosondes large discrepancies are obtained, which, for example, are shown in Fig. 8 from (Yao et al., 2014). Differences are seen not only in critical frequencies, but also in a profile of the topside part although in general density distribution throughout the profile provides conformity with the TEC(obs) for the account of the plasmaspheric part.
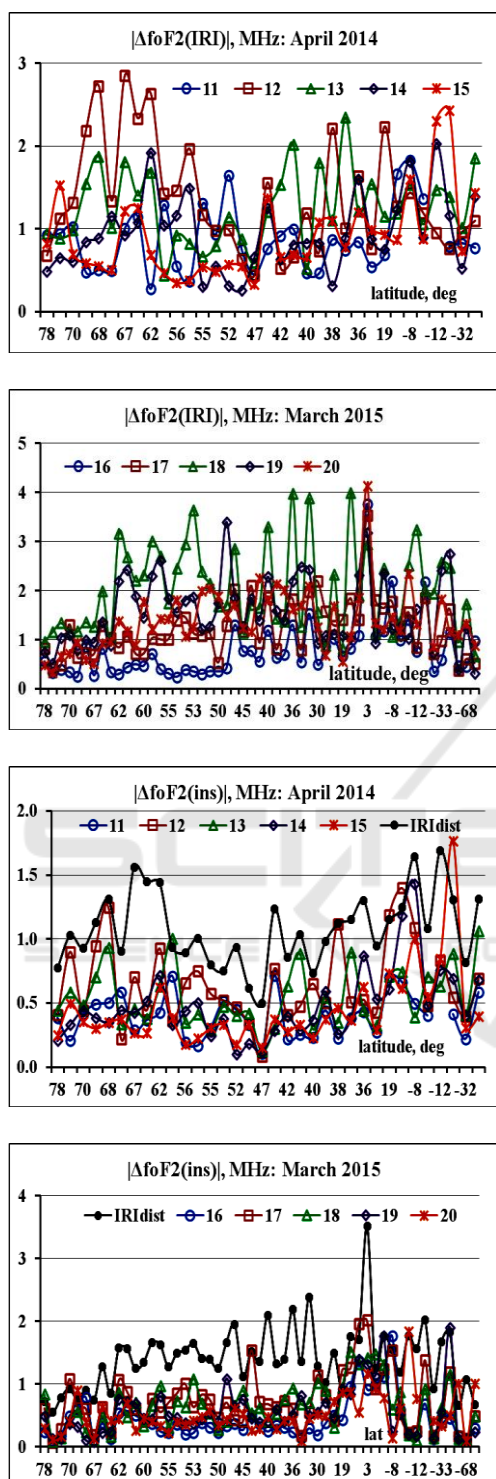
Figure 7: Details of deviation comparison in the disturbed periods.
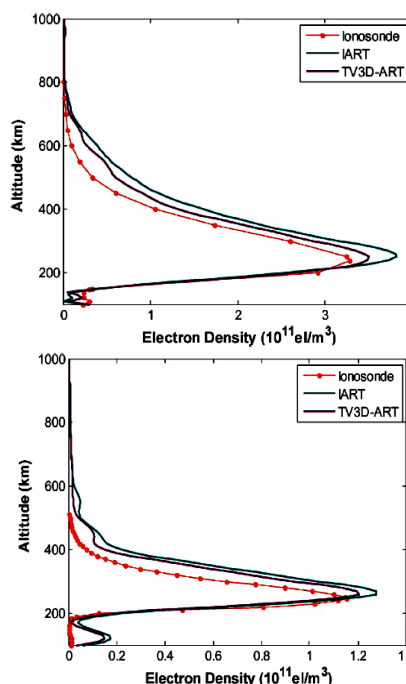
Figure 8: Conformity of assimilation profiles with the data of vertical sounding (from Yao et al., 2014).

4 INTERNET POSSIBILITIES OF USAGE OF THE LOW ORBIT SATELLITES DATA

By the end of the 20th century, data from different satellites began to play a larger role in the study of the ionosphere and radio propagation in it. One of the achievements of the 21st century is a creation of database of satellite CHAMP (http://isdc.gfz-potsdam.de/), which includes the value of the electron density at altitudes near the maximum height hmF2. Currently, this array also covers virtually one cycle of solar activity (2000-2011). Even earlier, similar data were provided by a series of satellites DMSP (http:// cindispace. utdallas.edu/ DMSP/ dmsp_data_at_utdallas.html). Since 2006, the huge amount of data was obtained by satellite COSMIC (http://tacc.cwb.gov.tw/en/). One of the goals of the simulation is to coordinate the model N(h)-profile and experimental TEC(obs). The IRI-Plas model (Gulyaeva, 2011) provides adaptation to TEC(obs), but the obtained profiles do not always ensure the coincidence with the plasma frequency, measured at the low orbit satellites. As shown in (Maltseva, 2014), adapting the model to the plasma frequency of one or two satellites gives values TEC(sat), not equal to TEC(obs). In this paper, the

difference Δ(TEC(sat)) = TEC(obs)-TEC(sat) was attributed to a plasmaspheric part of the profile and introduced coefficient K(PL), modifying this part of the profile so that the TEC of the modified profile is equal to TEC(obs). This factor is a multiplier, which the density of the profile at the upper limit (20,000 km) is multiplied by. Examples of profiles of the station Juliusruh in April 2001 have been shown that if the difference Δ(TEC(sat)) is positive then the coefficient K(PL) may be greater or less than 1. When K(PL)> 1 the profile may have nonphysical shape. When K(PL)<0 it is necessary to suppose density on the upper limit equal to zero, since it cannot be negative. TEC for such a profile may differ from the TEC(obs). This indicates a need for testing a plasmaspheric part of the profile. To do this, in this paper the model of (Ozhogin et al., 2012), based on the experimental data RPI (Radio Plasma Imager) of satellite IMAGE, was used. This model was developed in a range of L-shells from 1.6 to 4, so this test cannot be carried out for the station Juliusruh, as its L-shell does not fall in this range. Example of test is given for the station Ascension Island.
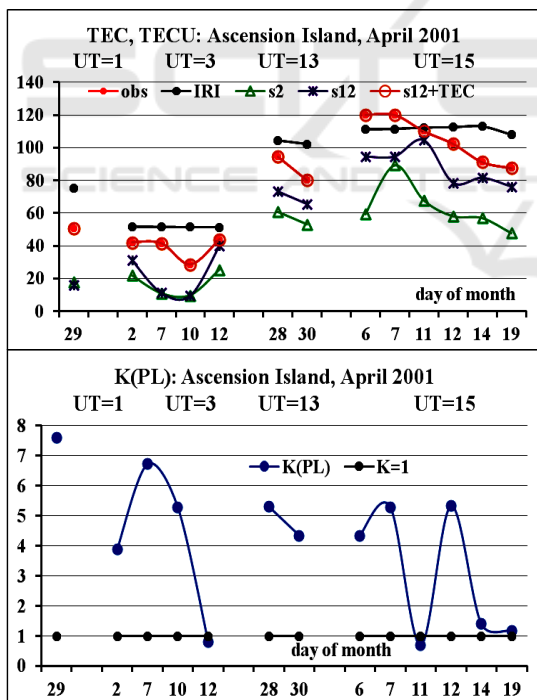
Figure 9: Comparison of values of TEC for various options of calculation and corresponding coefficients K(PL).

This example makes it possible to show the uncertainty of profiles associated with both the

shape of the profile, and with the uncertainty of value of TEC(obs), given by various global maps. Comparison of TEC for that station for the calculation of various options is given in Fig. 9 during moments of flight of the satellite CHAMP over the station. The horizontal axis represents the days of the month. Time of observation is shown at the top of the graph. Red dots on the top panels show the observed values, the black dots are the values for the original (without adaptation) model IRI. Green triangles belong to profiles of models adapted to foF2(obs) and fne(sat2), violet asterisks indicate the TEC for the profile, which is the starting point for modifications. Orange circles show the TEC for profile modified by the coefficient K(PL). The lower panel shows the corresponding coefficients K(PL).

This situation is typical for all the stations, only values of the difference between the TEC may vary depending on the latitude. Interestingly, the N(h)-profiles passing through fne(sat), give more lower values TEC(sat) than TEC(obs). The modification results in full compliance with the TEC(obs) using K(PL) from the lower panel. Fig. 10 shows the N(h)-profiles for one of the cases (April 12, UT = 3). Profile is represented for clarity in two parts: from the beginning of the ionosphere to the height of 2,000 km and from an altitude 2,000 km to an altitude of 20,000 km.

Fig. 10 includes the profile of the original model (black dots), for which the TEC(IRI) exceeds the TEC(obs), the profile calculated for a model adapted to foF2(obs) and TEC(obs) and shown by purple diamonds (mark "All"), profiles passing through fne(CHAMP) and foF2(obs). These profiles cannot always build. They are shown with blue crosses, and there are only in two panels. Profiles going through foF2(obs) and fne(DMSP) are shown by green triangles. They are built for all cases. Large red dots show fne(sat) on the top panels. Small red dots show the values of the model RPI on the bottom panels. A plasmaspheric part of all profiles is close to the model of RPI. Profile s12+PL, providing TEC(JPL)=44 TECU, in the upper panel, does not pass through the plasma frequency. The second panel shows the profiles for UPC map with TEC(UPC) = 31.8 TECU. In the profile "All", the topside part was decreased, but the plasmaspheric part was increased. It can be seen that the profile s12 + PL passes through fne(DMSP), but again there is no passage through fne(CHAMP).
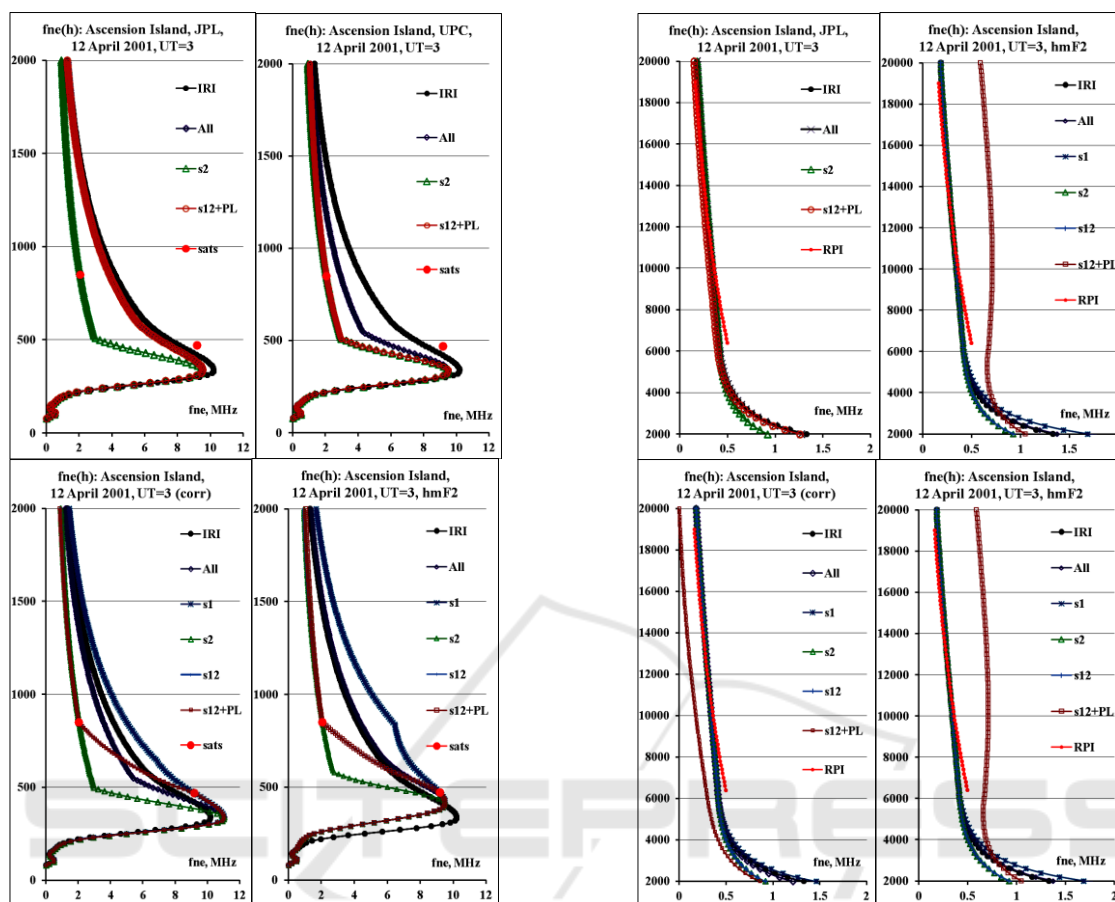
Figure 10: An illustration of conformity between model N(h)-profiles and observed TEC.

We attempted to modify the profile in two directions: to increase foF2(obs) (third panel) or hmF2 (fourth panel) in order to pass the profile through fne(CHAMP). In both cases, the profile has gone through fne(CHAMP), but the TEC of these profiles are greatly increased. In case of increase of foF2(obs), difference $\Delta(TEC(sat))$ was negative, resulting in a zero value at the upper limit of profile. In the second case, the topside part was not changed much. This led to a positive difference and an increase of the plasmaspheric density. These results lead to the important conclusion that to disambiguate N(h)-profile it is necessary to specify more precisely the values of TEC and shape of the topside profile because the plasmaspheric part is close to the existing model.

.

5 INTERNET POSSIBILITIES OF USAGE OF EMPIRICAL MODELS OF THE IONOSPHERE

Presence of huge array of data and approximation methods has led to possibility of creating of empirical models of the ionosphere which with success are used for forecasting of its state. Among set of empirical models which are disposed on the Internet, the IRI model is one of the most demanded and most dynamically developing (http://irimodel.org). In this century it has undergone some updates: IRI2001, IRI2007, 2010, 2012 (Bilitza, 2001; Bilitza, Reinisch, 2008; Bilitza et al., 2014).

Main attention focuses on the correspondence of model parameters to experimental values. In this study, a comparison of the model with observed data

was held including data of stations which have appeared on the Internet only recently (since 2013). It allowed us to obtain results in a global scale (Fig. 5, 7).
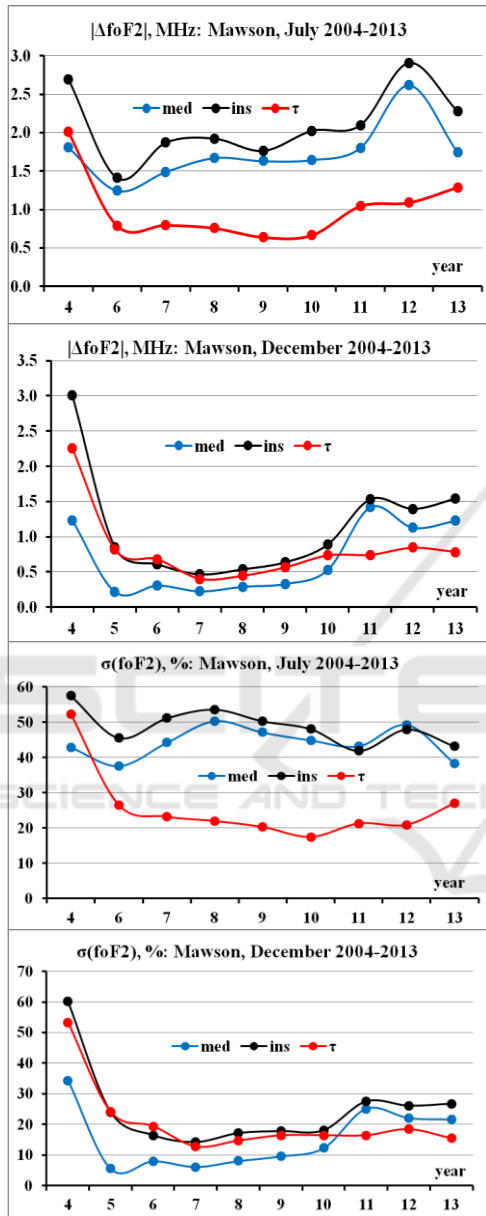
Figure 11: An estimate of accuracy of the model IRI according to data of the Antarctic station Mawson.

Of great interest is evaluation of the IRI model possibilities in the high latitudes of the southern hemisphere in connection with the project GRAPE (De Franceschi, Candidi, 2012). In this work, the first results were obtained according to data of the station Mawson. Fig. 11 shows the absolute and relative deviations of July and December for all the

years with available data. Black dots show deviations from day to day, blue dots – deviations of medians and red dots – deviations of foF2 values, calculated with usage of the TEC and τ(med).

It is evident that in July (winter) deviations of curves with marks "med" and "ins" are significantly exceed the values typical for the northern hemisphere. Using the TEC and τ(med) improves the situation, except for 2004. Moreover, this Figure does not include the values for 2005 in connection with abnormal values of foF2, shown in Fig. 12 requiring additional study (the top panel). One reason may be an insufficient quantity of data: the lower panel shows the deviation |ΔfoF2| along with the number of days reduced by 10 times.
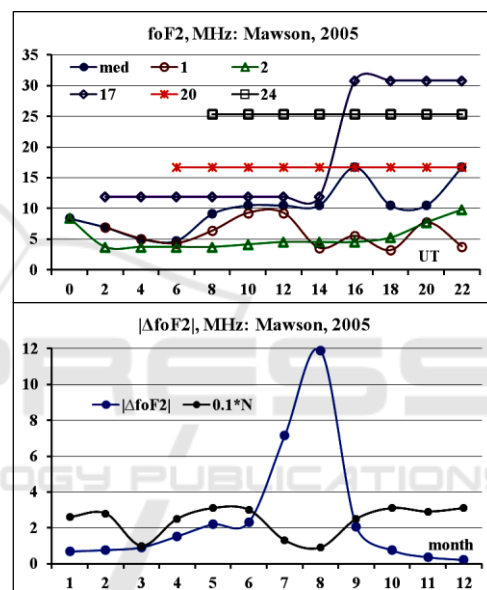
Figure 12: An illustration of the abnormal behavior of foF2 at the station Mawson in 2005.

In December results are comparable with the values typical for the northern hemisphere.

In (Maltseva et al., 2012; 2013; Maltseva, 2014) a lot of attention was paid to the comparison of different empirical models of foF2 and TEC (Gulyaeva, 2011; Hoque, Jakowski, 2011; Jakowski et al., 2011). In addition to these results, a huge volume of data has been used in (Maltseva et al., 2014; 2015) for comparison, covering more than 10-15 stations in different regions of the globe and several years. Despite this, an unambiguous answer was not obtained.

Great expectations are linked to a database of satellites COSMIC. The COSMIC EDP data are obtained from the COSMIC Data Analysis and Archive Center (CDAAC) at University Corporation for Atmospheric Research (UCAR). COSMIC RO

measurements and products (such as electron density profiles) can be available from the Taiwan Analysis Center for COSMIC (TACC, http://tacc.cwb.gov.tw/en/) and the COSMIC Data Analysis and Archive Center (CDAAC, http://www.cosmic.ucar.edu/cdaac/).

6 CONCLUSIONS

Only a few examples illustrate the possibility of obtaining new results using the resources of the Internet. For ionospheric studies, the most important are databases of the vertical sounding, measurements of TEC by high-orbit navigation satellites, measurements of plasma frequency by low-orbit satellites, data of solar and geomagnetic conditions. The obtained results show the large possibilities of use of resources of the Internet for study of the ionosphere and the representation of conditions of propagation of radio-waves. A series of new knowledge in this area was obtained.

But there is another side to such use: (1) it is not always possible to reconcile different data to each other because of their inaccuracies and ambiguities, (2) there is a danger in the access closing of certain countries, as it may be in an emergency situation.

ACKNOWLEDGEMENTS

REFERENCES

Bilitza, D., 2001. International Reference Ionosphere, *Radio Sci*., *36(2), 261-275.*

Bilitza, D., Reinisch, B.W., 2008. International Reference Ionosphere 2007: Improvements and New Parameters. *Adv. Space Res., 42, 599-609.*

Bilitza, D., Altadill, D., Zhang, Y., Mertens, C., Truhlik, V., Richards, P., McKinnell, L.-A., Reinisch, B., 2014. The International Reference Ionosphere 2012 – a model of international collaboration, *J. Space Weather Space Clim*., *4, A07, 12p. DOI: 10.1051/swsc/2014004.*

De Franceschi, G., Candidi, M., 2013. GRAPE, GNSS Research and Application for Polar Environment,

Expert Group of SCAR, *Annals of Geophysics*, *Special Issue 56. 2. P0215*; *Edited by Giorgiana, doi:10.4401/ag-6366.*

Fuller-Rowell, T., Araujo-Pradere, E., Minter, C., Codrescu, M., Spencer, P., Robertson, D., Jacobson, A.R., 2006. A new data assimilation product from the Space Environment Center characterizing the ionospheric total electron content using real-time GPS data US-TEC, *Radio Sci. 41, RS6003, doi: 10.1029/2005RS003393.*

Gulyaeva, T.L., 2011. Storm time behavior of topside scale height inferred from the ionosphere-plasmosphere model driven by the F2 layer peak and GPS-TEC observations. *Adv. Space Res., 47, 913-920.*

Hoque, M.M., Jakowski, N., 2011. A new global empirical NmF2 model for operational use in radio systems. *Radio Sci., 46, RS6015, 1-13.*

Houminer, Z., Soicher H., 1996. Improved short –term predictions of foF2 using GPS time delay measurements. *Radio Sci., 31(5), 1099-1108.*

Jakowski, N., Hoque, M.M., Mayer, C., 2011. A new global TEC model for estimating transionospheric radio wave propagation errors. *Journal of Geodesy, 85(12), 965-974.*

Khattatov, B., Murphy, M., Gnedin, M., Sheffel, J., Adams, J., Cruickshank, B., Yudin, V., Fuller-Rowell, T., Retterer, J. 2005. Ionospheric nowcasting via assimilation of GPS measurements of ionospheric electron content in a global physics-based time-dependent model. *Q.J.R.Meteorol. Soc*., *131, 3543–3559.*

Maltseva, O., 2014. Choice of the definition method for the total electron content to describe the conditions in the ionosphere. *Proceedings of Third International Conference on Telecommunications and Remote Sensing, Luxemburg, Grand Duchy of Luxemburg, 26-27 June 2014, 51-61.*

Maltseva, O.A., Mozhaeva, N.S., Nikitenko, T.V., 2014. Validation of the Neustrelitz Global Model according to the low latitude ionosphere. *Adv. Space Res.,54, 463–472, http://dx.doi.org/10.1016/j.asr.2013.11.005.*

Maltseva, O.A., Mozhaeva, N.S., Nikitenko, T.V., 2015. Comparative analysis of two new empirical models IRI-Plas and NGM (the Neustrelitz Global Model). *Adv. Space Res.,55, 2086–2098.*

Maltseva, O., Mozhaeva N., Vinnik E., 2013. Validation of two new empirical ionospheric models IRI-Plas and NGM describing conditions of radio wave propagation in space. *Proceedings of Second International Conference on Telecommunications and Remote Sensing, Noordwijkerhout, The Netherlands, 11-12 July, 109-118.*

Maltseva, O., Mozhaeva, N., Zhbankov, G., 2012. A new model of the International Reference Ionosphere IRI for Telecommunication and Navigation Systems. *Proceedings of the First International Conference on Telecommunication and Remote Sensing, 129-138.*

Maltseva, O.A., Poltavsk, O.S., Schlyupkin, A.S., 2007. The IRI model residual difference and the new method

of N(h)-profile determination. *Acta Geophysica, 55, 441-458.*

McNamara, L.F., 1985. The use of total electron density measurements to validate empirical models of the ionosphere. *Adv. Space Res., 5(7), 81-90.*

McNamara, L.F., 2006. Quality figures and error bars for autoscaled Digisonde vertical incidence ionograms. *Radio Sci., 41, RS4011, doi:10.1029/2005RS003444.*

Ozhogin, P., Tu, J., Song, P., Reinisch, B.W., 2012. Field-aligned distribution of the plasmaspheric electron density: An empirical model derived from the IMAGE RPI measurements, *J. Geophys. Res., 117, A06225.*

Reinisch, B.W., Galkin, I.A., Khmyrov, G.M., Kozlov, A.V., Bibl, K., Lisysyan, I.A., Cheney, G.P., Huang, X., Kitrosser, D.F., Paznukhov, V.V., Luo, Y., Jones, W., Stelmash, S., Hamel, R., Grochmal, J., 2009. The New Digisonde for Research and Monitoring Applications. *Radio Sci.,RS004115.*

URSI Atlantic Radio Science Conference, 18-22 May 2015, ExpoMeloneras, Grand Canaria, http://www.at-rasc.com

Yao, Y., Tang, J., Chen, P., Zhang, S., Chen, J., 2014. An Improved Iterative Algorithm for 3-D Ionospheric Tomography Reconstruction. *IEEE Transactions on Geoscience and Remote sensing, 52, 8.*

Zabotin, N.A., Wright, J.W., Bullett, T.W., Zabotina, L.Ye., 2005. Dynasonde 21: principles of data processing, transmission and web service. *11 International Ionospheric Effects Symposium, Alexandria, USA, 3-5 May 2005, 7B51-7B58.*